Chapter 4

Numerical Solutions to the Multigroup Diffusion Equation

Multigroup diffusion methods are the workhorse of industrial nuclear reactor neutronics modeling and simulation. The primary reason for this is that there has been a great deal of in developing efficient, accurate, and robust numerical solution techniques. In this chapter we will first detail how almost all neutron diffusion problems reduce to the repeated solution of steady-state, one-group neutron diffusion problems. We then discuss some spatial discretization techniques: the classic finite difference method and the more efficient nodal methods. We then discuss acceleration of iterative techniques to solve neutron diffusion problems, primarily coarse-mesh finite difference.

4.1 Time-dependent multigroup diffusion

In the previous chapter we derived the time-dependent multigroup diffusion equation for the scalar flux of neutrons in group g, $\phi_g(x,y,z,t)$,

$$\frac{1}{\bar{v}_g}\partial_t\phi_g - \nabla\cdot D_g\nabla\phi_g + \Sigma_{\mathrm{r}g}\phi_g = \sum_{g'=1,g'\neq g}^{G}\Sigma_{\mathrm{s},g'\to g}\phi_{g'} + \chi_g\sum_{g'=1}^{G}\bar{\nu}\Sigma_{\mathrm{f}g'}\phi_{g'} + Q_g, \quad (4.1)$$

for $\vec{r} = (x,y,z)^{\mathrm{t}} \in V$, $t \in [0,\infty)$, and $g \in [1,G]$. The boundary and initial conditions are of the form

$$\mathcal{A}_{1g}\phi_g(x,y,z,t) + \mathcal{B}_g\hat{n}\cdot\nabla\phi_g(x,y,z,t) = \mathcal{C}_g, \qquad \vec{r}\in\partial V, \quad (4.2)$$

where $\hat{n}$ is the outward normal at the boundary point (x,y,z) and

$$\phi_g(x,y,z,0) = \Phi_g(x,y,z). \quad (4.3)$$

To solve Eq. (4.1) in time-dependent problems we will typically employ an implicit time discretization. A common implicit time integrator is the backward Euler method, sometimes called the implicit Euler method. In this approach we integrate Eq. (4.1) over a time step Δt. We usually write the beginning of the time step as time t^n and the end of the time step as $t^{n+1} = t^n + \Delta t$. In the backward Euler method we evaluate all the terms except the time derivative at time t^{n+1}. Upon integration of Eq. (4.1) over Δt we get

In this equation $\phi_g^n(x, y, z) \approx \phi_g(x, y, z, t^n)$ and we have implicitly assumed that the material properties do not vary over time or that they can be evaluated at t^{n+1} as well. Note that in our notation $\phi_g^0 = \Phi_g(x, y, z)$. Rearranging this equation we get an equation that looks like a steady-state equation:

$$-\nabla \cdot D_g \nabla \phi_g^{n+1} + \Sigma_{\mathrm{r}g}^* \phi_g^{n+1} = \sum_{g'=1, g' \neq g}^{G} \Sigma_{\mathrm{s},g' \to g} \phi_{g'}^{n+1} + \chi_g \sum_{g'=1}^{G} \bar{\nu} \Sigma_{\mathrm{f}g'} \phi_{g'}^{n+1} + Q_g^*, \tag{4.5}$$

where we have defined effective absorption and source terms to be

(4.6)

Equation (4.5) is known as the quasi-steady form of the multigroup neutron diffusion equation because it has the form of a steady-state equation with the time-dependence coming from the source and absorption terms. The procedure for solving a time-dependent problem from $t = 0$ to $t = t_{\mathrm{final}}$ in this manner is given by

1.

2.

3.

The upshot is that to solve a time dependent problem we need to solve many steady state problems. This will be true for almost any implicit time discretization technique. The difference between backward Euler and other approaches,

e.g., Crank-Nicolson or BDF-2, is the form of the effective absorption and source terms.

4.2 k-Eigenvalue Problems and Power Iteration

Finding the k-eigenvalue and fundamental mode of a nuclear system is also a problem of interest. For these problems we remove all sources and have no incoming neutrons from the boundary, and divide the fission term by an eigenvalue k. The multigroup diffusion k-eigenvalue problem is then

$$-\nabla \cdot D_g \nabla \phi_g + \Sigma_{\mathrm{r}g}\phi_g = \sum_{g'=1, g' \neq g}^{G} \Sigma_{\mathrm{s},g' \to g}\phi_{g'} + \frac{\chi_g}{k}\sum_{g'=1}^{G} \bar{\nu}\Sigma_{\mathrm{f}g'}\phi_{g'}, \tag{4.7}$$

for $\vec{r} = (x, y, z)^{\mathrm{t}} \in V$ and $g \in [1, G]$. The boundary conditions are of the form, for Marshak conditions,

$$\frac{1}{4}\phi_g(x, y, z) + \frac{D_g}{2}\hat{n} \cdot \nabla \phi_g(x, y, z) = 0, \qquad \vec{r} \in \partial V. \tag{4.8}$$

A straightforward, and common approach to solving the k-eigenvalue system is power iteration. In this approach we have a guess for $\phi_g(x, y, z)$ that we call $\phi_g^{(l)}(x, y, z)$ and compute a fission source F_g:

and then solve the steady-state problem

(4.9)

for $\phi_g^{(l+1)}$. Then we compute the approximation to k as

This iteration process is repeated until the eigenvalue approximation converges.

In k-eigenvalue problems, as in time-dependent diffusion problems, we are left with solving steady-state diffusion problems repeatedly. We will describe power iteration in more detail when we have a fully discrete system.

4.3 α-Eigenvalue Problems

In an α-eigenvalue problem we are interested in finding the α eigenvalue with the largest real part (i.e., the rightmost in the complex plane). These problems are of interest for safety calculations where one is interested in how the neutron population will change in time after an initial layer. Therefore, one desires the value of α with the largest real part for which there is a nontrivial solution to

$$-\nabla \cdot D_g \nabla \phi_g + \left(\Sigma_{\mathrm{r}g} + \frac{\alpha}{\bar{v}_g}\right)\phi_g = \sum_{g'=1, g' \neq g}^{G} \Sigma_{\mathrm{s},g' \to g}\phi_{g'} + \chi_g \sum_{g'=1}^{G} \bar{\nu}\Sigma_{\mathrm{f}g'}\phi_{g'}, \quad (4.10)$$

for $\vec{r} = (x, y, z)^{\mathrm{t}} \in V$ and $g \in [1, G]$. As in the k-eigenvalue problem, the boundary conditions are of the form, for Marshak conditions,

$$\frac{1}{4}\phi_g(x, y, z) + \frac{D_g}{2}\hat{n} \cdot \nabla \phi_g(x, y, z) = 0, \qquad \vec{r} \in \partial V. \quad (4.11)$$

The procedure for finding the dominant α eigenvalue and eigenfunction, one can use the so-called α search technique. In this process we solve a specialized k-eigenvalue problem with an approximate value of α, $\alpha^{(l)}$, given by

(4.12)

for $\vec{r} = (x, y, z)^{\mathrm{t}} \in V$ and $g \in [1, G]$ and the same boundary conditions. Notice that if the k-eigenvalue in this problem is 1, then $\alpha^{(l)}$ is an α eigenvalue. We cannot say if it is the largest magnitude value, but we do know that it is an α eigenvalue. We need to implement some search procedure to find an α. One possible approach is to first find the criticality of the system: if the system is subcritical then the rightmost eigenvalue has a real part less than 0, if it is supercritical then the rightmost α eigenvalue has a positive real part, and a critical system has the rightmost value of α equal to 0.

Given that part of the search procedure requires solving k-eigenvalue problems, once again the workhorse calculation is solving steady-state neutron diffusion problems.

4.4 Iteration for Multigroup Diffusion Problems

In the previous sections we have motivated the fact that the common neutron diffusion problems we would like to solve involve solving several steady-state diffusion problems. These problems have the general form

$$-\nabla \cdot D_g \nabla \phi_g + \Sigma_{\mathrm{r}g}\phi_g = \sum_{g'=1, g' \neq g}^{G} \Sigma_{\mathrm{s},g' \to g}\phi_{g'} + \breve{Q}_g, \quad (4.13)$$

for $\vec{r} = (x, y, z)^{\mathrm{t}} \in V$ and $g \in [1, G]$. We have defined a new source term that depends on whether we are solving a time step of a time-dependent problem or a power iteration in a k-eigenvalue problem:

(4.14)

The boundary conditions are of the general form given by Eq. (4.2). To numerically solve this type of problem we need to compute the scalar flux for each group. This is typically done via an iteration procedure. We begin with a guess for the solution that we call $\phi_g^{(0)}(x, y, z)$. We then solve the group 1 equation, the highest energy group, by solving the following equation with $m = 0$

(4.15)

We then use this solution to solve an equation for group 2:

(4.16)

This process is repeated, group by group, until we reach group G and solve the equation:

(4.17)

The iteration process where we solve a single-group at a time, starting at the highest energy, and then proceed lower in energy using the most recent value for the higher-energy scalar fluxes is known as Gauss-Seidel iteration because it resembles the classic iterative method for solving linear systems. The benefit of this approach is that if there is only down-scattering in the system (i.e., $\Sigma_{\mathrm{s},g' \to g} = 0$ when $g < g'$), the solution will converge in one complete iteration.

In many nuclear systems there is no up-scattering into any of the groups except for the thermal groups. For such a system, the groups with no up-scatter will converge in a single iteration and then the one only needs to iterate over the thermal groups multiple times until convergence. Later we will talk about ways to accelerate the convergence of the thermal groups.

Before moving on, let's pause for a moment to look at where we are. We started with a general multigroup diffusion problem (either time-dependent or eigenvalue) and then proceeded to show that each of these reduced to the solution of several steady-state multigroup diffusion problems. We have just shown that the solution of steady-state mulitgroup diffusion problems reduce to the solution of several single-group, steady-state diffusion problems. This is where we will focus our attention next.

4.5 The Finite Difference Method

We have shown that to solve any multigroup diffusion problem of interest, we need to repeatedly solve a diffusion problem of the form

$$\nabla \cdot \vec{J} + \Sigma_{\mathrm{a}} \phi = Q, \tag{4.18}$$

where the net current density is given by Fick's law

$$\vec{J} = -D \nabla \phi. \tag{4.19}$$

The boundary conditions we use are

$$\mathcal{A}\phi(x,y,z) + \mathcal{B}\hat{n} \cdot \nabla \phi(x,y,z) = \mathcal{C}, \qquad \vec{r} \in \partial V. \tag{4.20}$$

where $\hat{n}$ is the outward normal at the boundary point (x,y,z). In Eq. (4.18) the value of D, Σ_{a} and Q are appropriately chosen for the problem as shown in previous sections. For instance, in a time-dependent problem Σ_{a} would include the fission term. Also, Q will have the scattering source from other groups along with fission and fixed source contributions.

To solve Eq. (4.18) we will partition our domain V into a set of rectangular parallelepipeds called zones and assume that the domain V is also a rectangular parallelepiped of size $X \times Y \times Z$. For now we will assume that the size of the parallelepipeds is the same everywhere with dimensions $h_x \times h_y \times h_z$. We will index the zones with three indices corresponding to the zone number in each of the directions x, y, and z. This means that zone ijk contains all the points $x \in ((i-1/2)h_x, (i+1/2)h_x)$, $y \in ((j-1/2)h_y, (j+1/2)h_y)$, and $z \in ((i-1/2)h_z, (k+1/2)h_z)$, and $i = 1, \ldots, I$, $j = 1, \ldots, J$, $k = 1, \ldots, K$. The

number of zones in each direction is given by

Furthermore, we are interested in finding the average scalar flux in each zone, and we assert that in each zone the D, Σ_{a}, and Q are constant. The average scalar flux for zone ijk is given by

(4.21)

where

The material properties in each zone are also denoted by the three subscripted indices, just as the scalar flux is, so that $\Sigma_{\mathrm{a},ijk}$ is the macroscopic absorption cross-section in zone ijk. The reason we are interested in the average scalar flux over a zone is that under the condition of constant cross-sections in a zone, the total reaction rate density in each zone is given by $\Sigma_{R,ijk}\phi_{ijk}$ where R is a type of reaction. Therefore, we can easily compute important quantities of interest for reactor analysis (e.g., power rate densities) using the average scalar flux.

We now consider a generic zone away from a boundary (i.e., $i \neq 1, I$, $j \neq 1, J$, and $k \neq 1, K$). In this zone we will replace the derivatives with differences over the zone and the middle of each face. For example, the derivative of J_x in zone ijk will be approximated using a finite difference formula

(4.22)

where

This approximation allows us to write Eq. (4.18) as

$$\frac{J_x(x_{i+1/2}, y_j, z_k) - J_x(x_{i-1/2}, y_j, z_k)}{h_x} + \frac{J_y(x_i, y_{j+1/2}, z_k) - J_y(x_i, y_{j-1/2}, z_k)}{h_y} + \frac{J_z(x_i, y_j, z_{k+1/2}) - J_z(x_i, y_j, z_{k-1/2})}{h_z} + \Sigma_{\mathrm{a},ijk}\phi_{ijk} = Q_{ijk}. \quad (4.23)$$

We then use Fick's law to write the net current on each face using a finite difference. To do this we will interpret the cell average scalar flux as living at the center of the zone. We then can write the net current at a face as, for example,

(4.24)

The problem is that we don't know what $\phi(x_{i-1/2}, y_j, z_k)$ is in terms of zone average scalar fluxes. To determine this quantity we note that on the other side of the face, the current can be calculated as

(4.25)

Furthermore, at the interface we want the net current density to be continuous because this is the interface condition for a diffusion problem. Therefore, we set Eq. (4.24) equal to Eq. (4.25) to get

(4.26)

We can solve this equation for $\phi(x_{i-1/2}, y_j, z_k)$ as

(4.27)

Plugging this into the original equation for $J_x(x_{i-1/2}, y_j, z_k)$ we get

(4.28)

where the diffusion coefficient $\hat{D}_{(i-1/2)jk}$ is the harmonic mean of the diffusion coefficient on both sides of the interface:

(4.29)

Putting this result into Eq. (4.23) we get the discrete equations for a zone away from the boundary:

$$
\begin{aligned}
&- \frac{\hat{D}_{(i+1/2)jk}(\phi_{(i+1)jk} - \phi_{ijk}) - \hat{D}_{(i-1/2)jk}(\phi_{ijk} - \phi_{(i-1)jk})}{h_x^2} \\
&\quad - \frac{\hat{D}_{i(j+1/2)k}(\phi_{i(j+1)k} - \phi_{ijk}) - \hat{D}_{i(j-1/2)k}(\phi_{ijk} - \phi_{i(j-1)k})}{h_y^2} \\
&- \frac{\hat{D}_{ij(k+1/2)}(\phi_{ij(k+1)} - \phi_{ijk}) - \hat{D}_{ij(k-1/2)}(\phi_{ijk} - \phi_{ij(k-1)})}{h_z^2} + \Sigma_{\mathrm{a},ijk}\phi_{ijk} = Q_{ijk}.
\end{aligned}
\tag{4.30}
$$

The last part of the derivation concerns the boundary conditions. To demonstrate how the boundary conditions are invoked we will look at the equation for $i = 1$ leaving the current on the boundary undefined:

$$
\begin{aligned}
&- \frac{\hat{D}_{(3/2)jk}(\phi_{2jk} - \phi_{1jk}) - h_x J_x(0, y_j, z_k)}{h_x^2} \\
&\quad - \frac{\hat{D}_{1(j+1/2)k}(\phi_{1(j+1)k} - \phi_{1jk}) - \hat{D}_{1(j-1/2)k}(\phi_{1jk} - \phi_{1(j-1)k})}{h_y^2} \\
&- \frac{\hat{D}_{1j(k+1/2)}(\phi_{ij(k+1)} - \phi_{1jk}) - \hat{D}_{1j(k-1/2)}(\phi_{ijk} - \phi_{1j(k-1)})}{h_z^2} + \Sigma_{\mathrm{a},1jk}\phi_{1jk} = Q_{1jk}.
\end{aligned}
\tag{4.31}
$$

The boundary condition tells us that

Note that Fick's law tells us that

so that the boundary condition becomes

Rearranging this boundary condition we get,

(4.32)

In this case, to get $\phi(0, y, z)$ we will linearly extrapolate between ϕ_{1jk} and ϕ_{2jk} as

(4.33)

to get the current on the boundary as

(4.34)

Therefore, at the boundary we can simply plug in $J_x(0, y, z)$ from Eq. (4.34). There is a slight problem, however, for Dirichlet boundary conditions because these conditions will have $\mathcal{B} = 0$. In this case we go back to our finite difference formula and use

(4.35)

4.5.1 The Finite Difference Equations

Now that we have a closed system of equations to solve to compute the scalar fluxes ϕ_{ijk} we can write the system of equations as a linear system

where the unknowns $\vec{\phi}$ are the ϕ_{ijk}'s arranged as a vector, the matrix $\mathbf{A}$ is defined by Eq. (4.30), and the righthand side contains the source terms coming from both the boundary and Q_{ijk}'s. This system can be solved by any number of linear solvers. Though given that it is likely to be large system for a 3-D problem, iterative methods are usually preferred.

4.6 Finite Difference Solutions to Time-Dependent, Multigroup Problems

Now that we have discretized the single-group, fixed-source, steady-state diffusion equation, we can put all this together to solve time-dependent multigroup

problems. To do this we will define a problem that we want to solve with known values of D_g, $\Sigma_{\mathrm{r}g}$, $\Sigma_{\mathrm{s},g'\to g}$, and Q_g for $g = 1 \dots G$ along with the appropriate boundary conditions. To solve this problem each time step of the problem will involve solving a steady-state multigroup problem. This problem will have iterations if there is fission or up-scattering. An algorithm for doing this is given next.

Data: D_g, $\Sigma_{\mathrm{r}g}$, $\Sigma_{\mathrm{s},g'\to g}$, $\bar{\nu}\Sigma_{\mathrm{f}g}$, and Q_g for $g = 1 \dots G$; Boundary Conditions; step size: Δt, number of time steps: N_t, initial condition: $\vec{\phi}_g$
Result: Scalar flux $\vec{\phi}_g$ for each group
for *step* $\in [0, N_t]$ **do**
  while *not converged* **do**
    for $g \in [1, G]$ **do**
      Compute $\Sigma^*_{\mathrm{r}g}$ and Q^* from Eq. (4.6);
      Compute $\breve{Q}_g$ from Eq. (4.14);
      Solve 1-group diffusion problem with finite differences;
      Compute the down-scattering source, and update the fission source for all group greater than g;
    end
  end
  Update $\vec{\phi}_g$ with new solution;
end

Algorithm 1: Algorithm for solving multigroup time dependent problems

The `while` loop where the groups are converged is a Gauss-Seidel approach as we talked about earlier. Also, the 1-group diffusion problem we solve should bring the fission term for group g, $\chi_g \bar{\nu}\Sigma_{\mathrm{f}g}\phi_g$ to the left-hand side for stability.

4.7 Finite Difference Solutions to k-eigenvalue, Multigroup Problems

To solve a multi-group k-eigenvalue problem, we will have two types of iterations during the solve. The outer iterations are the power iterations that we mentioned above to find the k-eigenvalue. Inside each power iteration we have to iterate to find the solution to the stead-state, fixed source multi-group problem. The algorithm is outlined below:

Data: D_g, $\Sigma_{\mathrm{r}g}$, $\Sigma_{\mathrm{s},g'\to g}$, $\bar{\nu}\Sigma_{\mathrm{f}g}$ for $g = 1 \dots G$; Acceptable Boundary Conditions
Result: Fundamental mode scalar flux $\vec{\phi}_g$ for each group and eigenvalue k
while $k^{(l+1)}$, $\phi_g^{(l+1)}$ *are not converged* **do**
  while *groups are not converged* **do**
    for $g \in [1, G]$ **do**
      Compute $\breve{Q}_g$ from Eq. (4.14);
      Solve 1-group diffusion problem with finite differences;
      Compute the down-scattering source;
    end
    Update $\vec{\phi}_g^{(l+1)}$ and $k^{(l+1)}$ with new solution;
  end
end

Algorithm 2: Algorithm for solving multigroup k-eigenvalue problems

This algorithm will incur at least G single-group steady state solves per inner iteration. Moreover, therefore it is important to have a fast single-group solver to compute the eigenvalue.

4.8 Finite Difference Solutions to α-eigenvalue, Multigroup Problems

This case is even more expensive because to find the α-eigenvalue we need to solve many k-eigenvalue problems. The procedure we will use is a secant-method to find the α-eigenvalue. In particular, we solve Eq. (4.12) and compute the change in k per change in α, the slope between the two points as

(4.36)

We then use this slope and the approximation that $k(\alpha)$ is linear to get updated guess for α to test in our modified k-eigenvalue problem as

(4.37)

We repeat this process until k is sufficiently close to 1 or the maximum number of iterations is reached. For the first iteration we approximate the slope using a finite difference.

One drawback to this method is that we cannot guarantee that we are finding the rightmost value of α in the complex plane. There is no known method that can overcome this difficulty.

4.9 Nodal Methods for Multigroup Diffusion

Another approach to solving multigroup diffusion equations are nodal methods. In nodal methods one integrates over two of the three directions in space and solves the remaining 1-D multigroup diffusion problem to a high degree of accuracy. The method we will detail is the Nodal Expansion Method or NEM, that solves the 1-D problem with a high-order finite element technique. The benefit to nodal methods is that they require many fewer unknowns to get the same accuracy finite difference methods. As in our development of finite difference methods we will work on a regular grid of rectangular parallelepipeds, all of which have the same dimensions $h_x \times h_y \times h_z$.

Consider the 3-D, multigroup diffusion equation in a homogeneous material with a spatial varying source, i.e, the multigroup diffusion equation for a single zone in the mesh.

$$\partial_x J_{xg} + \partial_y J_{yg} + \partial_z J_{zg} + \Sigma_{\mathrm{r}g}\phi_g = Q_g, \qquad x \in \left(-\frac{h_x}{2}, \frac{h_x}{2}\right) \quad y \in \left(-\frac{h_y}{2}, \frac{h_y}{2}\right), \quad z \in \left(-\frac{h_z}{2}, \frac{h_z}{2}\right), \tag{4.38}$$

$$J_{xg} = -D_g \partial_x \phi_g, \qquad J_{yg} = -D_g \partial_y \phi_g, \qquad J_{zg} = -D_g \partial_z \phi_g, \tag{4.39}$$

$$Q_g = \sum_{g'=1, g\neq g}^{G} \Sigma_{\mathrm{s},g'\to g}\phi_{g'} + S_g(x,y,z), \tag{4.40}$$

where S_g contains the fixed and fission sources. We will solve this equation with Brunner boundary conditions:

$$\mathcal{A}^-_{xg}\phi_g\left(-\frac{h_x}{2}, y, z\right) + \mathcal{B}^-_{xg}\partial_x\phi_g\left(-\frac{h_x}{2}, y, z\right) = \mathcal{C}^-_{xg}, \qquad \mathcal{A}^+_{xg}\phi_g\left(\frac{h_x}{2}, y, z\right) + \mathcal{B}^+_{xg}\partial_x\phi_g\left(\frac{h_x}{2}, y, z\right) = \mathcal{C}^+_{xg}, \tag{4.41}$$

and similar boundary conditions for y and z.

What we care about in this problem is the average scalar flux over the domain because this is directly related to the reaction rate in each region. To get an equation for the average scalar flux we integrate over the entire domain and divide by $h_x h_y h_z$ to get

where the average scalar flux is

$$\bar{\phi}_g = \frac{1}{h_x h_y h_z} \int_{-h_x/2}^{h_x/2} dx \int_{-h_y/2}^{h_y/2} dy \int_{-h_z/2}^{h_z/2} dz\, \phi_g(x,y,z), \tag{4.43}$$

and the face-averaged currents are defined as

$$\hat{J}_{xg}(x) = \frac{1}{h_y h_z} \int_{-h_y/2}^{h_y/2} dy \int_{-h_z/2}^{h_z/2} dz\, J_{xg}(x,y,z), \qquad \hat{J}_{yg}(y) = \frac{1}{h_x h_z} \int_{-h_x/2}^{h_x/2} dx \int_{-h_z/2}^{h_z/2} dz\, J_{yg}(x,y,z), \tag{4.44}$$

We cannot just solve Eq. (4.42) because we need a relation between $\bar{\phi}$ and the face averaged currents. The finite difference equations accomplish this using simple relationships. We will instead use a different approach to find $\bar{\phi}$: we will solve a 1-D problem to find this relation.

Let us average Eq. (4.38) over y and z to get

(4.45)

(4.46)

where the leakage in the y and z directions is defined as

with

$$\breve{J}_{yg}(x,y) = \frac{1}{h_z} \int_{-h_z/2}^{h_z/2} dz\, J_{yg}(x,y,z), \qquad \breve{J}_{zg}(x,z) = \frac{1}{h_y} \int_{-h_y/2}^{h_y/2} dz\, J_{zg}(x,y,z). \tag{4.48}$$

Equation (4.45) is a one-dimensional diffusion equation in slab geometry that we will approximate the solution to as a quartic polynomial

(4.49)

where the expansion parameters a_{ng} and the average scalar flux in the node, $\bar{\phi}_g$ are unknown; this is $5G$ unknowns. The functional form of the expansion is defined so that

We will also write the source as function of x using the same quartic expansion:

(4.50)

in this case the expansion coefficients, q_{ng} would be known.

We also need to stipulate the form of the transverse leakage terms, $L_{yg}(x)$ and $L_{zg}(x)$. In each of these terms we will approximate the net current density on a face as a quadratic in x as, for the y direction,

(4.51)

This form is chosen so that the average over x of $\breve{J}_{yg}$ is equal to the face-averaged current:

We pick the other two expansion parameters by asserting that the average over

the faces in the adjacent zones also gives the face-averaged current:

and

where the index $i-1$ or $i+1$ indicates we are referring to the interface current in the zone to the left or right respectively. Solving these three equations gives

$$l_{1g}^{\pm} = \frac{\hat{J}_{i+1,yg}\left(\frac{\pm h_y}{2}\right) - \hat{J}_{i-1,yg}\left(\frac{\pm h_y}{2}\right)}{2h_x} \tag{4.52}$$

$$l_{2g}^{\pm} = \frac{\hat{J}_{i+1,yg}\left(\frac{\pm h_y}{2}\right) - 2h_x\hat{J}_{yg}\left(\frac{\pm h_y}{2}\right) + \hat{J}_{i-1,yg}\left(\frac{\pm h_y}{2}\right)}{6h_x^2}. \tag{4.53}$$

The quadratic expansion in the z direction for the transverse leakage is identical.

We will now find the expansion parameters for the quartic form of the scalar flux in the zone. To find the expansion parameters we plug Eq. (4.49) into Eq. (4.42) to get

(4.54)

where

Using Fick's law we can simplify the current terms to get

(4.55)

(4.56)

This gives us G equations. We can get $2G$ more equations using the boundary conditions. The boundary condition at $x = -h_x/2$ gives

(4.57)

which simplifies to

(4.58)

Similarly, we get for the right boundary condition

(4.59)

In total, this gives us $3G$ equations. To get the remaining equations we will integrate the linear and quadratic expansion functions against Eq. (4.45). The integral of linear expansion function, x/h_x, times Eq. (4.45) gives us

The integral of the quadratic expansion function against Eq. (4.45) gives

We now have $5G$ equations and $5G$ unknowns and we can solve for the scalar flux in the zone. We will now do a simple example to build our intuition for how this will work in practice.

4.9.1 Example: One-group, 1-D slab, Fixed Source

To show how the nodal process works, let us consider a 1-D slab with a fixed source and vacuum boundaries in the x direction. In this case the transverse leakages will be zero, and we will have 5 equations to solve. These equations are

(4.62)

$$\frac{1}{4}\left(\bar{\phi}-\frac{a_1}{2}+\frac{a_2}{2}\right)-\frac{D}{2}\left(\frac{a_1}{h_x}-\frac{3a_2}{h_x}+\frac{a_3}{2h_x}-\frac{a_4}{5h_x}\right)=0, \tag{4.63}$$

$$\frac{1}{4}\left(\bar{\phi}+\frac{a_1}{2}+\frac{a_2}{2}\right)+\frac{D}{2}\left(\frac{a_1}{h_x}+\frac{3a_2}{h_x}+\frac{a_3}{2h_x}+\frac{a_4}{5h_x}\right)=0, \tag{4.64}$$

$$-\frac{a_3 D}{2h_x}+\frac{1}{12}a_1 h_x\Sigma_{\mathrm{a}}-\frac{1}{120}a_3 h_x\Sigma_{\mathrm{a}}=0, \tag{4.65}$$

and

$$-\frac{a_4 D}{5h_x}+\frac{1}{20}a_2 h_x\Sigma_{\mathrm{a}}-\frac{1}{700}a_4 h_x\Sigma_{\mathrm{a}}=0. \tag{4.66}$$

The solution to this system for the average scalar flux is

$$\bar{\phi}=\frac{Q}{\Sigma_{\mathrm{a}}}-\frac{40DQ\left(\Sigma_{\mathrm{a}}h_x^2+42D\right)}{\Sigma_{\mathrm{a}}\left(1680D^2\Sigma a h_x+40D\Sigma_{\mathrm{a}}^2h_x^3+180D\Sigma_{\mathrm{a}}h_x^2+\Sigma_{\mathrm{a}}^2h_x^4+1680D^2\right)}. \tag{4.67}$$

The odd expansion parameters are 0:

and the other expansion parameters are

$$a_2=-\frac{2Qh_x^2\left(\Sigma_a h_x^2+140D\right)}{\Sigma_a^2h_x^3\left(40D+h_x\right)+60D\Sigma_a h_x\left(28D+3h_x\right)+1680D^2}, \tag{4.68}$$

$$a_4=-\frac{70Q\Sigma_a h_x^4}{\Sigma_a^2h_x^3\left(40D+h_x\right)+60D\Sigma_a h_x\left(28D+3h_x\right)+1680D^2}. \tag{4.69}$$

To see how the nodal method approximates the scalar flux in the node, we will plot the solution to this problem along with the analytic solution for $D=Q=\Sigma_{\mathrm{a}}=1$ for several different values of h_x. With these material properties, h_x is also the number of diffusion lengths in the zone. In Fig. (4.1)

the solution for a number of different values of h_x is shown. With a small value of h_x the solution from the nodal method is virtually indistinguishable from the analytic solution in the figure. As h_x gets larger the solution looks less like the analytic solution and the $h_x = 100$ solution has the nodal solution give a fundamentally different behavior than the analytic solution. When we look at

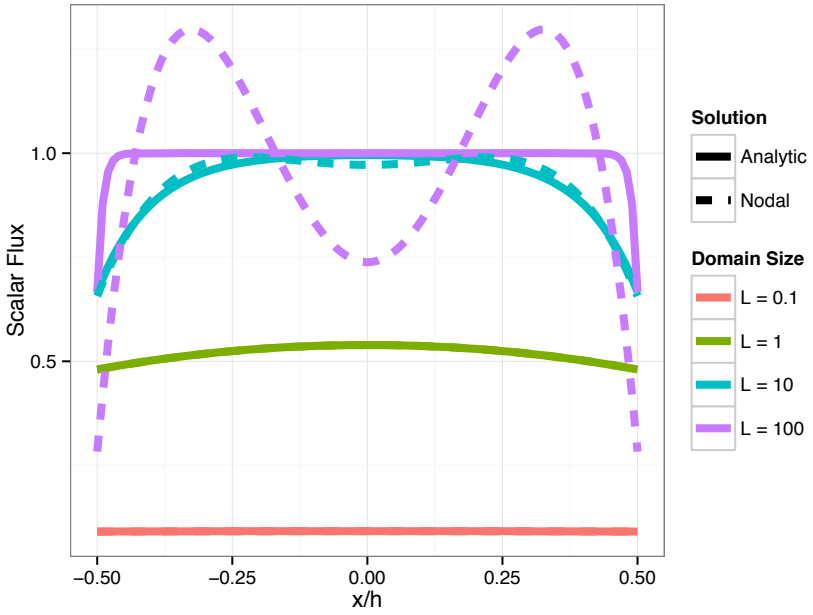

Figure 4.1: The nodal reconstructed solution compared with the analytic solution to a slab diffusion problem with $D = \Sigma_a = Q = 1$ and different values of h_x.

the error in the zone-averaged flux, however, we see where the nodal method shines. The convergence rate for the method in this problem is observed to be $O(h_x^{6.5})$. This is shown by the gray line in Fig. 4.2. Below $h_x \approx 0.1$, the nodal approximation agrees to the analytic solution to machine precision. Another salubrious phenomenon we not is that although the error grows as the slab gets thicker, it seems to stagnate at a level around 0.1% on this problem as the analytic solution goes to $\bar{\phi} = 1$.

4.9.2 Example: One-group, 1-D slab, k-eigenvalue

We will now increase the complexity of our example problem slightly by making it a k-eigenvalue problem. One again we will consider a 1-D slab, this time,

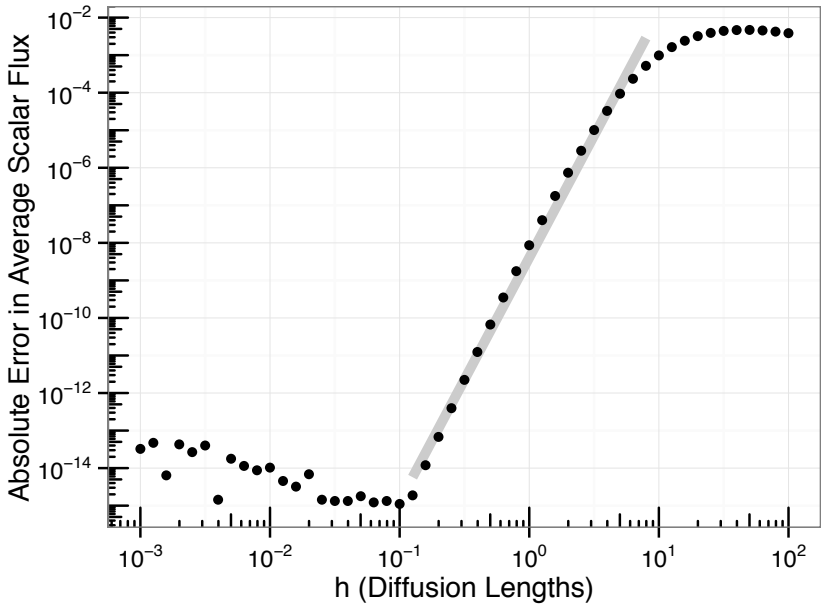

Figure 4.2: The nodal approximation to the zone-averaged scalar flux converges to the transport solution at rapid rate: the slope of the gray line is 6.5.

however, we will need to iterate to get the solution and the eigenvalue. Once again the transverse leakages will be zero. We will perform power iteration on the nodal equations using the iteration index l. The equations that need to be solved at each iteration are

(4.70)

$$\frac{1}{4}\left(\bar{\phi} - \frac{a_1^{(l+1)}}{2} + \frac{a_2^{(l+1)}}{2}\right) - \frac{D}{2}\left(\frac{a_1^{(l+1)}}{h_x} - \frac{3a_2^{(l+1)}}{h_x} + \frac{a_3^{(l+1)}}{2h_x} - \frac{a_4^{(l+1)}}{5h_x}\right) = 0, \tag{4.71}$$

$$\frac{1}{4}\left(\bar{\phi} + \frac{a_1^{(l+1)}}{2} + \frac{a_2^{(l+1)}}{2}\right) + \frac{D}{2}\left(\frac{a_1}{h_x} + \frac{3a_2}{h_x} + \frac{a_3^{(l+1)}}{2h_x} + \frac{a_4^{(l+1)}}{5h_x}\right) = 0, \tag{4.72}$$

$$-\frac{a_3^{(l+1)}D}{2h_x} + \frac{1}{12}a_1^{(l+1)}h_x\Sigma_{\mathrm{a}} - \frac{1}{120}a_3^{(l+1)}h_x\Sigma_{\mathrm{a}} = \frac{1}{12}a_1^{(l)}h_x\bar{\nu}\Sigma_{\mathrm{f}} - \frac{1}{120}a_3^{(l)}h_x\bar{\nu}\Sigma_{\mathrm{f}}, \tag{4.73}$$

and

$$-\frac{a_4^{(l+1)}D}{5h_x} + \frac{1}{20}a_2^{(l+1)}h_x\Sigma_{\mathrm{a}} - \frac{1}{700}a_4^{(l+1)}h_x\Sigma_{\mathrm{a}} = \frac{1}{20}a_2^{(l)}h_x\bar{\nu}\Sigma_{\mathrm{f}} - \frac{1}{700}a_4^{(l)}h_x\bar{\nu}\Sigma_{\mathrm{f}}. \tag{4.74}$$

We will solve these equations using an initial guess for the ϕ expansion, solve for an updated ϕ, and then compute

and then before proceeding set

where $\vec{\phi} = (\bar{\phi}, a_1, a_2, a_3, a_4)^{\mathrm{t}}$. We continue the iterations until we converge in both k and $\bar{\phi}$.

Using this approach to solve a 1-D slab problem with $D = \Sigma_{\mathrm{a}} = \bar{\nu}\Sigma_{\mathrm{f}} = 1$ and vacuum boundaries gives errors of less than 1 pcm (i.e., less than 10^{-5}) compared with the analytic diffusion solution. The k-eigenvalue estimated by the nodal method converges at a rate of $O(h_x^{1.87})$ as shown in Fig. (). We note that in this problem the dominance ratio (the ratio of the largest eigenvalue to the second largest) goes to 1 as $h_x \to 0$.

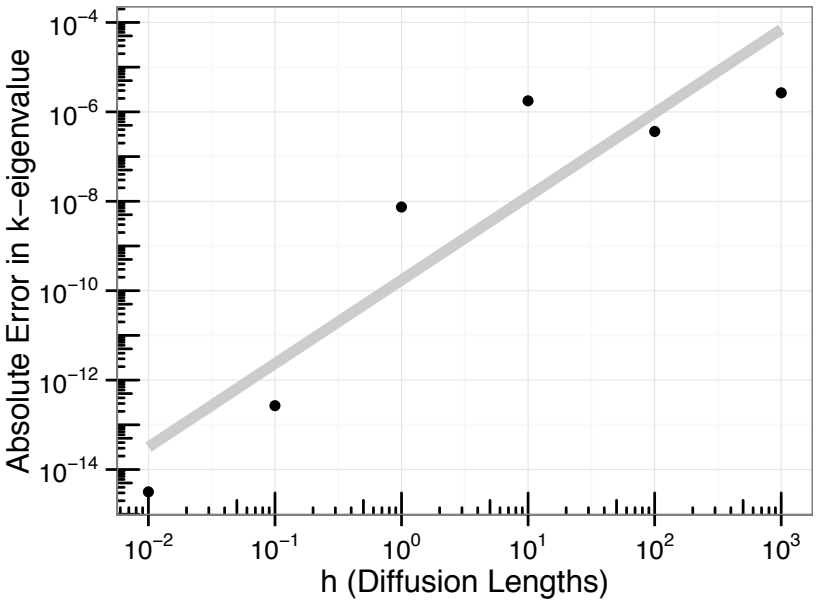

Figure 4.3: The convergence of the k-eigenvalue calculated by the nodal approximation to the diffusion equation is close to second-order in the number of nodes. The slope of the gray line is 1.87.

4.9.3 Example: One-group, 1-D heterogeneous slab

The next extension is to extend our problem to have multiple zones with different values for the cross-sections. The difference between this and our other examples is the fact that now the solution to one node feeds into the neighboring nodes. To do this we need to calculate the incoming current from one node to another. For a given node, the exiting current on each side of the node is

We then use this to replace the boundary conditions in the x-direction for the node. Now the boundary conditions for the nodes depend on the solution to other nodes. This suggests the following iteration procedure: we guess an initial value for the node expansion coefficients, compute the boundary conditions for each node, and then compute new nodal expansion coefficients, and continue until the solution converges.

For a fixed-source, heterogeneous problem the nodal solution converges quickly as the value of h is decreased. To demonstrate this we solve a two-region problem where a slab of width 3 has a value of $D = \Sigma_a = 1$ and $Q = 0$ for $x \in (-1.5, 0)$, and $D = \Sigma_a = 0.5$ and $Q = 1$ for $x \in (0, 1.5)$ and vacuum conditions at the edge of the slab. We compute the error in the solution with varying node sizes by comparing with the solution with 400 nodes at 30 points within the slab. The convergence rate we observe is close to fifth order.

4.9.4 Example: Two-group, 1-D slab with two nodes

This example is particularly important because it forms the basis for some of the acceleration techniques we will discuss later. For this situation we will have

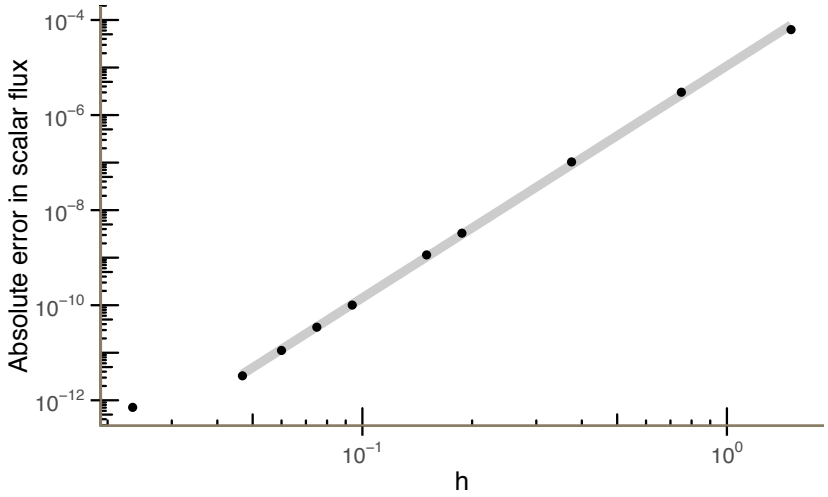

Figure 4.4: The convergence of the scalar flux calculated by the nodal approximation on a two-region heterogeneous problem. The slope of the gray line is about 4.9.

20 unknowns (5 for each node per group). We will denote the left node using the superscript L and the right node using R.The balance equations for the left and right nodes are

(4.77a)

(4.77b)

$$\Sigma_{\mathrm{r}2}^{\mathrm{L}}\bar{\phi}_2^{\mathrm{L}} + \frac{2\left(15a_{22}^{\mathrm{L}} + a_{42}^{\mathrm{L}}\right)D_2^{\mathrm{L}}}{5h_x^2} + \Sigma_{\mathrm{s}1\to 2}\bar{\phi}_1^{\mathrm{L}} = \bar{S}_2^{\mathrm{L}}, \tag{4.77c}$$

and

$$\Sigma_{\mathrm{r}2}^{\mathrm{R}}\bar{\phi}_2^{\mathrm{R}} + \frac{2\left(15a_{22}^{\mathrm{R}} + a_{42}^{\mathrm{R}}\right)D_2^{\mathrm{R}}}{5h_x^2} + \Sigma_{\mathrm{s}1\to 2}\bar{\phi}_1^{\mathrm{R}} = \bar{S}_2^{\mathrm{R}}. \tag{4.77d}$$

There will also be four equations to enforce that the exiting current from the left node is the same as the incoming current into the right node. For the

right node with have the following two equations for the left interface:

$$\frac{1}{4}\left(\bar{\phi}_g^{\mathrm{L}}+\frac{a_{1g}^{\mathrm{L}}}{2}+\frac{a_{2g}^{\mathrm{L}}}{2}\right)-\frac{D_g^{\mathrm{L}}}{2}\left(\frac{a_{1g}^{\mathrm{L}}}{h_x}+\frac{3a_{2g}^{\mathrm{L}}}{h_x}+\frac{a_{3g}^{\mathrm{L}}}{2h_x}+\frac{a_{4g}^{\mathrm{L}}}{5h_x}\right)= \frac{1}{4}\left(\bar{\phi}_g^{\mathrm{R}}-\frac{a_{1g}^{\mathrm{R}}}{2}+\frac{a_{2g}^{\mathrm{R}}}{2}\right)+\frac{D_g^{\mathrm{R}}}{2}\left(\frac{a_{1g}^{\mathrm{R}}}{h_x}-\frac{3a_{2g}^{\mathrm{R}}}{h_x}+\frac{a_{3g}^{\mathrm{R}}}{2h_x}-\frac{a_{4g}^{\mathrm{R}}}{5h_x}\right). \quad (4.77e)$$

Similarly, we have for the right interface of the left node, we have the condition that the incoming current from the right node is the same as the incoming current computed on the interface:

$$\frac{1}{4}\left(\bar{\phi}_g^{\mathrm{R}}-\frac{a_{1g}^{\mathrm{R}}}{2}+\frac{a_{2g}^{\mathrm{R}}}{2}\right)-\frac{D_g^{\mathrm{R}}}{2}\left(\frac{a_{1g}^{\mathrm{R}}}{h_x}-\frac{3a_{2g}^{\mathrm{R}}}{h_x}+\frac{a_{3g}^{\mathrm{R}}}{2h_x}-\frac{a_{4g}^{\mathrm{R}}}{5h_x}\right)= \frac{1}{4}\left(\bar{\phi}_g^{\mathrm{L}}+\frac{a_{1g}^{\mathrm{L}}}{2}+\frac{a_{2g}^{\mathrm{L}}}{2}\right)+\frac{D_g^{\mathrm{L}}}{2}\left(\frac{a_{1g}^{\mathrm{L}}}{h_x}+\frac{3a_{2g}^{\mathrm{L}}}{h_x}+\frac{a_{3g}^{\mathrm{L}}}{2h_x}+\frac{a_{4g}^{\mathrm{L}}}{5h_x}\right). \quad (4.77f)$$

Notice that these equations are the same as stating that the scalar flux and current are continuous at the interface.

Each node has two other equations for the interface we have not considered yet. For the left node, its left boundary must satisfy the boundary condition as

$$\mathcal{A}_{xg}^{-}\left(\bar{\phi}_g^{\mathrm{L}}-\frac{a_{1g}^{\mathrm{L}}}{2}+\frac{a_{2g}^{\mathrm{L}}}{2}\right)+\mathcal{B}_{xg}^{-}\left(\frac{a_{1g}^{\mathrm{L}}}{h_x}-\frac{3a_{2g}^{\mathrm{L}}}{h_x}+\frac{a_{3g}^{\mathrm{L}}}{2h_x}-\frac{a_{4g}^{\mathrm{L}}}{5h_x}\right)=\mathcal{C}_{xg}^{-}. \quad (4.77g)$$

The right boundary of the right node must satisfy the external boundary condition as

$$\mathcal{A}_{xg}^{+}\left(\bar{\phi}_g^{\mathrm{R}}+\frac{a_{1g}^{\mathrm{R}}}{2}+\frac{a_{2g}^{\mathrm{R}}}{2}\right)+\mathcal{B}_{xg}^{+}\left(\frac{a_{1g}^{\mathrm{R}}}{h_x}+\frac{3a_{2g}^{\mathrm{R}}}{h_x}+\frac{a_{3g}^{\mathrm{R}}}{2h_x}+\frac{a_{4g}^{\mathrm{R}}}{5h_x}\right)=\mathcal{C}_{xg}^{+}. \quad (4.77h)$$

Next, the equations for the integral of the linear boundary condition against the nodal diffusion equation gives

$$-\frac{a_{31}^{\mathrm{L}}D_1^{\mathrm{L}}}{2h_x}+\frac{1}{12}a_{11}^{\mathrm{L}}h_x\Sigma_{\mathrm{r1}}^{\mathrm{L}}-\frac{1}{120}a_{31}^{\mathrm{L}}h_x\Sigma_{\mathrm{r1}}^{\mathrm{L}}=\frac{h_x}{12}\left(\Sigma_{\mathrm{s2}\to1}^{\mathrm{L}}a_{12}^{\mathrm{L}}+q_{11}^{\mathrm{L}}\right)-\frac{h_x}{120}\left(\Sigma_{\mathrm{s2}\to1}^{\mathrm{L}}a_{32}^{\mathrm{L}}+q_{31}^{\mathrm{L}}\right), \quad (4.77i)$$

$$-\frac{a_{31}^{\mathrm{L}}D_1^{\mathrm{R}}}{2h_x}+\frac{1}{12}a_{11}^{\mathrm{R}}h_x\Sigma_{\mathrm{r1}}^{\mathrm{R}}-\frac{1}{120}a_{31}^{\mathrm{R}}h_x\Sigma_{\mathrm{r1}}^{\mathrm{R}}=\frac{h_x}{12}\left(\Sigma_{\mathrm{s2}\to1}^{\mathrm{R}}a_{12}^{\mathrm{R}}+q_{11}^{\mathrm{R}}\right)-\frac{h_x}{120}\left(\Sigma_{\mathrm{s2}\to1}^{\mathrm{R}}a_{32}^{\mathrm{R}}+q_{31}^{\mathrm{R}}\right) \quad (4.77j)$$

$$-\frac{a_{32}^{\mathrm{L}}D_2^{\mathrm{L}}}{2h_x}+\frac{1}{12}a_{12}^{\mathrm{L}}h_x\Sigma_{\mathrm{r1}}^{\mathrm{L}}-\frac{1}{120}a_{32}^{\mathrm{L}}h_x\Sigma_{\mathrm{r1}}^{\mathrm{L}}=\frac{h_x}{12}\left(\Sigma_{\mathrm{s1}\to2}^{\mathrm{L}}a_{11}^{\mathrm{L}}+q_{12}^{\mathrm{L}}\right)-\frac{h_x}{120}\left(\Sigma_{\mathrm{s1}\to2}^{\mathrm{L}}a_{31}^{\mathrm{L}}+q_{32}^{\mathrm{L}}\right) \quad (4.77k)$$

and

$$-\frac{a_{32}^{\mathrm{R}}D_2^{\mathrm{R}}}{2h_x}+\frac{1}{12}a_{12}^{\mathrm{R}}h_x\Sigma_{\mathrm{r2}}^{\mathrm{R}}-\frac{1}{120}a_{32}^{\mathrm{R}}h_x\Sigma_{\mathrm{rg}}^{\mathrm{R}}=\frac{h_x}{12}\left(\Sigma_{\mathrm{s1}\to2}^{\mathrm{R}}a_{11}^{\mathrm{R}}+q_{12}^{\mathrm{R}}\right)-\frac{h_x}{120}\left(\Sigma_{\mathrm{s1}\to2}^{\mathrm{R}}a_{31}^{\mathrm{R}}+q_{32}^{\mathrm{R}}\right). \quad (4.77l)$$

The final four equations that we need are those found from integrating the quadratic basis function against the nodal diffusion equation. These are

$$-\frac{a_{41}^{\mathrm{L}}D_1^{\mathrm{L}}}{5h_x}+\frac{1}{20}a_{21}^{\mathrm{L}}h_x\Sigma_{\mathrm{r1}}^{\mathrm{L}}-\frac{1}{700}a_{41}^{\mathrm{L}}h_x\Sigma_{\mathrm{r1}}^{\mathrm{L}}=\frac{h_x}{20}\left(\Sigma_{\mathrm{s2}\to1}^{\mathrm{L}}a_{22}^{\mathrm{L}}+q_{21}^{\mathrm{L}}\right)-\frac{h_x}{700}\left(\Sigma_{\mathrm{s2}\to1}^{\mathrm{L}}a_{42}^{\mathrm{L}}+q_{41}^{\mathrm{L}}\right), \tag{4.77m}$$

$$-\frac{a_{41}^{\mathrm{R}}D_1^{\mathrm{R}}}{5h_x}+\frac{1}{20}a_{21}^{\mathrm{R}}h_x\Sigma_{\mathrm{r1}}^{\mathrm{R}}-\frac{1}{700}a_{41}^{\mathrm{R}}h_x\Sigma_{\mathrm{r1}}^{\mathrm{R}}=\frac{h_x}{20}\left(\Sigma_{\mathrm{s2}\to1}^{\mathrm{R}}a_{22}^{\mathrm{R}}+q_{21}^{\mathrm{R}}\right)-\frac{h_x}{700}\left(\Sigma_{\mathrm{s2}\to1}^{\mathrm{R}}a_{42}^{\mathrm{R}}+q_{41}^{\mathrm{R}}\right), \tag{4.77n}$$

$$-\frac{a_{42}^{\mathrm{L}}D_2^{\mathrm{L}}}{5h_x}+\frac{1}{20}a_{22}^{\mathrm{L}}h_x\Sigma_{\mathrm{r2}}^{\mathrm{L}}-\frac{1}{700}a_{42}^{\mathrm{L}}h_x\Sigma_{\mathrm{r2}}^{\mathrm{L}}=\frac{h_x}{20}\left(\Sigma_{\mathrm{s1}\to2}^{\mathrm{L}}a_{21}^{\mathrm{L}}+q_{22}^{\mathrm{L}}\right)-\frac{h_x}{700}\left(\Sigma_{\mathrm{s1}\to2}^{\mathrm{L}}a_{41}^{\mathrm{L}}+q_{42}^{\mathrm{L}}\right), \tag{4.77o}$$

and

$$-\frac{a_{42}^{\mathrm{R}}D_2^{\mathrm{R}}}{5h_x}+\frac{1}{20}a_{22}^{\mathrm{R}}h_x\Sigma_{\mathrm{r2}}^{\mathrm{R}}-\frac{1}{700}a_{42}^{\mathrm{R}}h_x\Sigma_{\mathrm{r2}}^{\mathrm{R}}=\frac{h_x}{20}\left(\Sigma_{\mathrm{s1}\to2}^{\mathrm{R}}a_{21}^{\mathrm{R}}+q_{22}^{\mathrm{R}}\right)-\frac{h_x}{700}\left(\Sigma_{\mathrm{s1}\to2}^{\mathrm{R}}a_{41}^{\mathrm{R}}+q_{42}^{\mathrm{R}}\right). \tag{4.77p}$$

These equations form a linear system that we can solve for the solution of the scalar flux in each node. Using this solution we can compute the current at the interface between the two nodes.

4.10 Coarse Mesh Finite Difference Acceleration

Nodal methods for multigroup diffusion are powerful in that they can describe the diffusion solution to large problems using few unknowns. However, the number of iterations to compute the nodal solution increases at $O(N)$ where N is the number of nodes. Additionally, the computational cost of a single iteration increases at $O(N)$ because the number of unknowns is linearly related to the number of nodes. This means that we expect the time to solution to grow quadratically as the number of nodes increases. We see this in Figure 4.5 where the number of iterations and the time to solution is plotted on a two-region, slab problem. The growth in the time to solution is problematic because in a 3-D problem to refine the mesh uniformly, the number of nodes grows cubicly. Therefore, to double the resolution in a 3-D problem, we would expect a factor of $2^6 = 64$ increase in the time to solution.

To decrease the number of iterations, we look to acceleration schemes. Acceleration techniques look for methods to decrease the number of iterations in by performing an auxiliary calculation to enhance the convergence of the solution. In particular we will examine the coarse-mesh, finite difference (CMFD) acceleration technique. This method solves the diffusion equation on a coarse mesh using finite differences. The solution of such a diffusion equation can be very efficient, especially if the number of unknowns is small. In practice the CMFD method is used where the mesh is the same or coarser than the nodes in the problem.

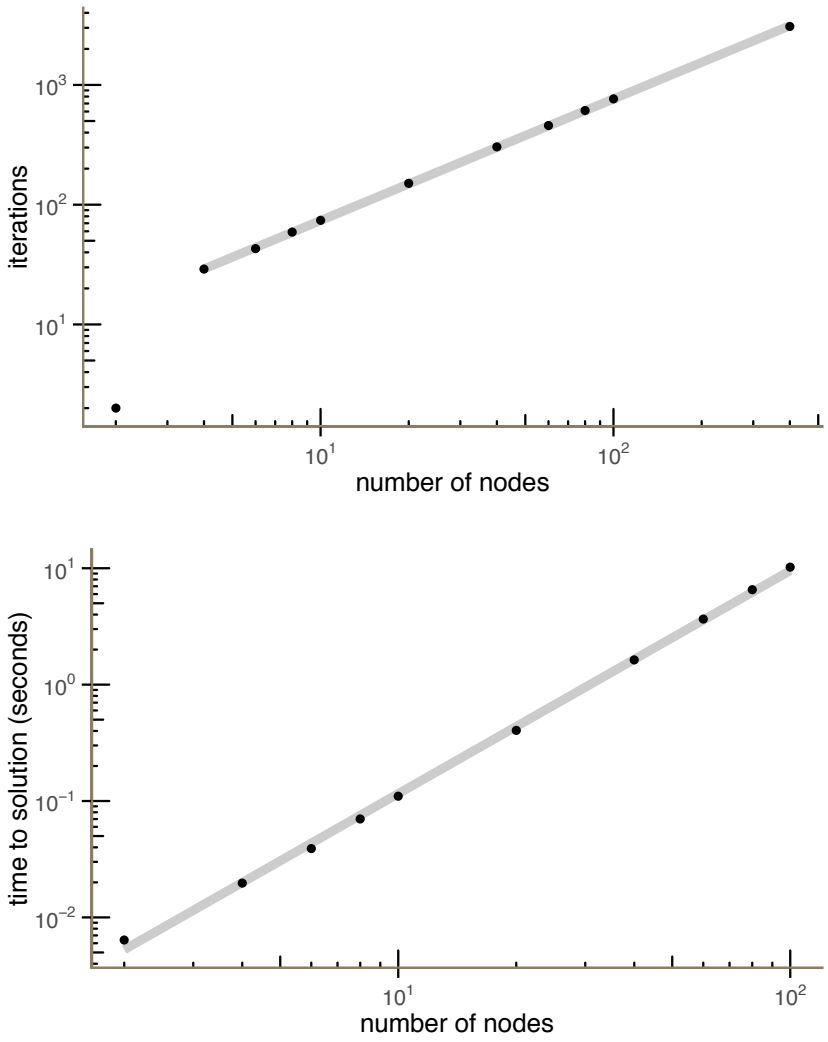

Figure 4.5: Top: The number of iterations increases at $O(N)$ where N is the number of nodes (the slope in this plot is 1.19). Bottom: The time increases quadratically in the number of nodes (the slope in this plot is 1.97).

For a fixed-source, single-group, problem, the CMFD method begins with the diffusion equation for the multigroup scalar flux integrated over a coarse zone denoted by the indices ijk:

$$\frac{J_x(x_{i+1/2},y_j,z_k)-J_x(x_{i-1/2},y_j,z_k)}{h_x}+ \frac{J_y(x_i,y_{j+1/2},z_k)-J_y(x_i,y_{j-1/2},z_k)}{h_y}+ \frac{J_z(x_i,y_j,z_{k+1/2})-J_z(x_i,y_j,z_{k-1/2})}{h_z}+\Sigma_{\mathrm{a},ijk}\phi_{ijk}=Q_{ijk}. \quad (4.78)$$

Instead of using the original version of Fick's law to write the current at the zone interfaces we add an additional term that looks like the average of scalar flux across the interface. For the current in the x direction we get, for constant mesh spacing,

(4.79)

We pick this form for the current at the interface so that we have an extra degree of freedom to enforce that the current used in the finite difference technique matches the current calculated by the nodal method. If we write the current averaged over the face of the zone by the nodal scheme as $\bar{J}_x^{\mathrm{node}}(x_{i-1/2})$, and equate this with the current in Eq. (4.79), and solve for $-\tilde{D}_{(i-1/2)jk}$ to get

(4.80)

To get the average current on the face of the zone, we add the positive and negative half-range currents on the edge of the zone:

(4.81)

where the positive moving current is calculated from the node to the left of the face and the negative moving current is calculated from the node to the right side of the face.

The iteration scheme for a fixed-source problem using CMFD can be described using an iteration index ℓ. We will denote values from the CMFD solution using the integral values and quantities from two-zone nodal calculations

using half-integral indices. For a given iteration we first compute the current at each interface. For the two-node problem the boundary conditions, in the x-direction, are given by specifying the boundary current using the values from the CMFD solve. For the interface at $x_{i+1/2}$ the boundary currents for the two-node problem are

$$J(x_{i-1/2})^{\ell+1/2} = -\hat{D}_{(i-1/2)jk}\frac{\phi^{\ell}_{ijk} - \phi^{\ell}_{(i-1)jk}}{h_x} - \tilde{D}^{\ell-1/2}_{(i-1/2)jk}\frac{\phi_{ijk} + \phi_{(i-1)jk}}{h_x}, \tag{4.82}$$

and the right boundary is

(4.83)

The solution to each two node problem then allows us to compute the correction factors at each interface:

(4.84)

We then solve the CMFD equations to update the zone-averaged scalar fluxes:

$$\begin{aligned}
&- \hat{D}_{(i+1/2)jk}\frac{\phi^{\ell+1}_{(i+1)jk} - \phi^{\ell+1}_{ijk}}{h_x^2} + \hat{D}_{(i-1/2)jk}\frac{\phi^{\ell+1}_{ijk} - \phi^{\ell+1}_{(i-1)jk}}{h_x^2} \\
&\quad - \tilde{D}^{\ell+1/2}_{(i+1/2)jk}\frac{\phi^{\ell+1}_{(i+1)jk} + \phi^{\ell+1}_{ijk}}{h_x^2} + \tilde{D}^{\ell+1/2}_{(i-1/2)jk}\frac{\phi^{\ell+1}_{ijk} + \phi^{\ell+1}_{(i-1)jk}}{h_x^2} + \\
&\quad - \hat{D}_{i(j+1/2)k}\frac{\phi^{\ell+1}_{i(j+1)k} - \phi^{\ell+1}_{ijk}}{h_y^2} + \hat{D}_{i(j-1/2)k}\frac{\phi^{\ell+1}_{ijk} - \phi^{\ell+1}_{i(j-1)k}}{h_y^2} \\
&\quad - \tilde{D}^{\ell+1/2}_{i(j+1/2)k}\frac{\phi^{\ell+1}_{i(j+1)k} + \phi^{\ell+1}_{ijk}}{h_y^2} + \tilde{D}^{\ell+1/2}_{i(j-1/2)k}\frac{\phi^{\ell+1}_{ijk} + \phi^{\ell+1}_{i(j-1)k}}{h_y^2} + \\
&\quad - \hat{D}_{ij(k+1/2)}\frac{\phi^{\ell+1}_{ij(k+1)} - \phi^{\ell+1}_{ijk}}{h_z^2} + \hat{D}_{ij(k-1/2)}\frac{\phi^{\ell+1}_{ijk} - \phi^{\ell+1}_{ij(k-1)}}{h_z^2} \\
&\quad - \tilde{D}^{\ell+1/2}_{ij(k+1/2)}\frac{\phi^{\ell+1}_{ij(k+1)} + \phi^{\ell+1}_{ijk}}{h_z^2} + \tilde{D}^{\ell+1/2}_{ij(k-1/2)}\frac{\phi^{\ell+1}_{ijk} + \phi^{\ell+1}_{ij(k-1)}}{h_z^2} + \\
&\qquad + \Sigma_{\mathrm{a},ijk}\phi^{\ell+1}_{ijk} = Q_{ijk}.
\end{aligned} \tag{4.85}$$

As $\ell \to \infty$ the scalar flux, ϕ^{ℓ}, will go to the node-averaged scalar flux that would be computed if we solved the entire system using the nodal method. This

procedure converges faster than the iterative strategy for computing the nodal fluxes discussed above because each step handles a different part of the error:

1.

2.

We have not said how to handle the problem boundaries in the CMFD iterations. For the two-node problems, when one of the nodes falls on the boundary we just use the specified boundary condition, in Brunner form, at that boundary. Then, for the CMFD calculation we specify the current at that boundary by using the nodal solution in the zone evaluated at the boundary.

The procedure can also work on multigroup problems. In such a situation one would solve nodal multigroup problems for the multigroup interface currents, and then solve a multigroup CMFD calculation to update the scalar fluxes.

4.10.1 CMFD for k-eigenvalue problems

The benefits of CMFD acceleration are most apparent in k-eigenvalue problems. In these problems we modify the solution procedure slightly so that the power iteration only takes place in the CMFD system. Once again we will use an iteration index ℓ for CMFD quantities and $\ell + 1/2$ for nodal quantities. The outline of the procedure is that we will solve two-node problems to compute the coupling between nodes using a known fission source, and then solve the CMFD equations to get the eigenvalue and fission source. This eigenvalue and fission source is then used to update the nodal problems in the next iteration. In our procedure we first compute the fission source for the nodal equations using the scalar flux from a CMFD calculation as, for the a nodal problem in x direction,

Notice that the CMFD scalar flux is only affecting the level of the fission source and not the shape. We then solve a fixed-source nodal, multigroup diffusion problem for the two-nodes around each interface as done above to get the net currents on each interface, $J(x_{i+1/2})^{\ell+1/2}$. Using these currents we compute the $\tilde{D}^{\ell+1/2}$. With these coefficients we then have a fully-specified diffusion k-eigenvalue problem. We solve this k-eigenvalue problem to get $\phi_g^{\ell+1}$ and $k^{\ell+1}$, and continue the iteration until the